

~~CONFIDENTIAL~~

JAN 20 1952

NACA RM L51K14a



RESEARCH MEMORANDUM

AERODYNAMIC CHARACTERISTICS AT SUPERSONIC SPEEDS OF A
SERIES OF WING-BODY COMBINATIONS HAVING CAMBERED
WINGS WITH AN ASPECT RATIO OF 3.5 AND A
TAPER RATIO OF 0.2

*Reference
May 16, 1957*

EFFECT AT $M = 1.60$ OF NACELLE SHAPE AND POSITION ON THE
AERODYNAMIC CHARACTERISTICS IN PITCH OF TWO WING-BODY
COMBINATIONS WITH 47° SWEPTBACK WINGS

By Lowell E. Hasel and John R. Sevier, Jr.

Langley Aeronautical Laboratory
Langley Field, Va.

CLASSIFIED DOCUMENT

This material contains information affecting the National Defense of the United States within the meaning of the espionage laws, Title 18, U.S.C., Secs. 793 and 794, the transmission or revelation of which in any manner to unauthorized person is prohibited by law.

NATIONAL ADVISORY COMMITTEE FOR AERONAUTICS

WASHINGTON
January 16, 1952

Date: *AM 76-18-57*

NACA Biobase

RN-127

CLASSIFICATION CHANGED

UNCLASSIFIED

To:

NACA LIBRARY

LANGLEY AERONAUTICAL LABORATORY
Langley Field, Va.

NATIONAL ADVISORY COMMITTEE FOR AERONAUTICS.

RESEARCH MEMORANDUM

AERODYNAMIC CHARACTERISTICS AT SUPERSONIC SPEEDS OF A
SERIES OF WING-BODY COMBINATIONS HAVING CAMBERED
WINGS WITH AN ASPECT RATIO OF 3.5 AND A
TAPER RATIO OF 0.2

EFFECT AT $M = 1.60$ OF NACELLE SHAPE AND POSITION ON THE
AERODYNAMIC CHARACTERISTICS IN PITCH OF TWO WING-BODY
COMBINATIONS WITH 47° SWEEPBACK WINGS

By Lowell E. Hasel and John R. Sevier, Jr.

SUMMARY

An investigation has been conducted in the Langley 4- by 4-foot supersonic pressure tunnel to determine the effect of a series of nacelles on the aerodynamic characteristics in pitch of a sweptback-wing - body combination. Nacelle shape and position were varied on a configuration with a 6-percent-thick wing having an aspect ratio of 3.5, a taper ratio of 0.2, and 47° of sweep at the quarter chord. Submerged nacelles were tested on this wing-body combination and also on a similar configuration with a 6-percent-thick wing having a thickened root section. Lift, drag, and pitching-moment results are presented at a Mach number of 1.60 and a Reynolds number of 2.7×10^6 based on the wing mean aerodynamic chord.

INTRODUCTION

A research program has been in progress at the Langley Aeronautical Laboratory to determine, at subsonic, transonic, and supersonic speeds, the effects of thickness ratio and sweep on the aerodynamic characteristics of a series of wing-body combinations. The cambered wings have an aspect ratio of 3.5 and a taper ratio of 0.2. The effects of sweep

at subsonic and transonic speeds are presented in reference 1. The effects of both sweep and thickness ratio on the aerodynamic characteristics in pitch at a Mach number of 1.60 are presented in references 2 and 3.

This paper presents the results of a nacelle investigation which was conducted on two wing-body combinations of this series. The nacelle shape and location were varied on a 6-percent-thick wing having the quarter-chord line sweptback 47° . Submerged nacelles were also tested on this configuration and on a similar configuration with a 6-percent-thick wing having a thickened root section. The root-section thickness ratio varied linearly from 12 percent at the body center line to 6 percent at the 40-percent-semispan station. Lift, drag, and pitching-moment results are presented at a Mach number of 1.60 and a Reynolds number of 2.7×10^6 based on the wing mean aerodynamic chord. The data of this report are presented without analysis to expedite publication.

SYMBOLS

\bar{c}	mean aerodynamic chord of wing (0.646 ft)
C_D	drag coefficient (D/qS)
ΔC_D	nacelle drag increment, drag-coefficient rise due to addition of nacelles to basic wing configuration
C_L	lift coefficient (L/qS)
C_m	pitching-moment coefficient about the quarter chord of the mean aerodynamic chord ($m/qS\bar{c}$)
D	drag
L	lift
M	Mach number
m	pitching moment
p	static pressure
q	dynamic pressure ($\frac{\gamma}{2} \rho M^2$)
S	wing-plan-form area (1.143 sq ft)

- α angle of attack, degrees
 γ ratio of the specific heats of air
 ψ angle of yaw, degrees

APPARATUS

Tunnel

These tests were conducted in the Langley 4- by 4-foot supersonic pressure tunnel which was originally powered by a 6,000-horsepower electric-drive system (reference 4). Recent modifications have increased the continuous horsepower rating to 45,000. Other modifications made at the same time included installing machined, flexible stainless-steel walls in place of the mild-steel flexible walls which form the nozzle and test section of the tunnel. The modifications have not affected the Mach number range which extends from 1.2 to 2.2. The maximum stagnation pressure has been increased from about 0.3 atmosphere to more than 2 atmospheres. At a Mach number of 1.60 the test section has a width of 4.5 feet, a height of 4.4 feet, and a region of uniform flow which is 7 feet long at the flexible walls. An external air-drying system supplies air of a sufficiently low dew point to prevent moisture condensation in the test section.

Models and Equipment

Wing body.- The basic wing-body model (fig. 1) consisted of a body formed by an ogival nose and a constant-diameter cylindrical section with a 6-percent-thick tapered wing having the quarter chord swept back 47° . Pertinent dimensions of the body and wing are given in figure 1. For one test the 6-percent-thick wing was replaced by a similar wing with a thickened root section. The thickness of the wing varied linearly from 12 percent at the fuselage center line to 6 percent at the 40-percent-semispan station and was constant over the remainder of the semispan. Ordinates for both wings are presented in table I.

Nacelles.- Two basic nacelle shapes were used during most of these tests. The open nacelle (fig. 2(a)) allowed straight-through air passage whereas the faired nacelle (fig. 2(b)) was closed at both entrance and exit. The three NACA series one nose inlets (reference 5) used on the open nacelle are illustrated in figure 2(a). Since the design inlet-velocity ratio increases rapidly as the length ratio of the nose inlet is increased (see reference 5), the inlet diameter ratio of the shorter nose inlets was reduced in designing the NACA 1-60-300 nose

inlet to avoid an excessively high inlet-velocity ratio. Pertinent dimensions of both faired and open nacelles are given in figure 2.

The open and faired nacelles were mounted at four vertical positions with respect to the wing chord plane as shown in figure 3 (the position designations denoted in fig. 3 are used throughout this paper). The nacelles were supported on each semispan by variable length struts which were swept forward 75° . The angle between the nacelle center line and the line formed by joining the top of the nacelle exit lip with the wing trailing edge at the nacelle station was constant at 15° for all open-nacelle tests. Nacelle strut details are shown in figure 2.

The submerged nacelle installations which were tested on the 6-percent-thick and thickened root wings are shown in figures 4(a) and 4(b). The frontal areas (including the area buried in the wing) of two submerged nacelles and of one open or faired nacelle (fig. 3) were equal.

Support system.- The model was sting-mounted in the tunnel as shown in figure 5. The attitude of the model was variable during a run in only a horizontal plane. A bent sting was therefore used so that the model could be tested, if desired, at combined angles of pitch and yaw (one attitude fixed, the other varied during a given run).

Force and pressure measurements.- Force data were obtained with an internally mounted six-component strain-gage balance. Pressure data were measured with a multiple-tube mercury manometer.

The models, balance, and associated indicating equipment were furnished by a U. S. Air Force contractor.

TESTS, CORRECTIONS AND ACCURACY

Tests

The results presented in this paper were obtained at a nominal Mach number of 1.60 and at a Reynolds number of 2.7×10^6 based on wing mean aerodynamic chord. The longitudinal characteristics were determined for an angle-of-attack range from -2° to 12° at zero yaw. The stagnation dew point was kept more negative than -25°F to prevent condensation effects on the flow in the test section. The configurations which were tested and the corresponding figure numbers in which the data are presented are listed in table II.

The strain-gage balance was calibrated prior to any model tests, and a check calibration was made while the tests were in progress.

During the initial phase of this check calibration, the balance constants agreed with those obtained from the initial calibration. As the check calibration progressed, however, the characteristics of the drag balance changed by 5 percent. Further checks of the drag balance indicated no further changes of the drag constant. All data obtained after the check calibration was made are based on the final calibration and are denoted by flagged symbols.

Corrections and Accuracy

The following table presents the approximate Mach number and flow angle variation along the test-section center line in the region of the model fuselage:

Mach number	±0.01
Flow angle variation in a horizontal plane	±0.1
Flow angle variation in a vertical plane	±0.1

No corrections have been applied to the data to account for these flow irregularities.

The data have been corrected for angular deflection of the model due to air loads. The model was at small negative yaw and roll angles (approx. -0.2° and -1.0° , respectively) during all of the tests, and no corrections have been applied to account for these effects.

The drag data have been corrected to reduce the base pressure to the free-stream value.

The estimated accuracies of the force data are as follows:

C_L	±0.005
C_D	±0.001
C_m	±0.001
α	±0.10

It should be mentioned that the tests were conducted so that the data presented for nacelle positions 2, 3, and 4 in figure 6 and all data presented in figure 8 were obtained from a consecutive series of tests in which the model configuration was not altered except to change the fore and aft portions of the nacelle configurations. Similarly, the data presented in figures 7 and 9 were obtained from two other series of consecutive tests. It is therefore thought that the small differences in the results are valid and are a result of the different nacelle configurations and not differences due to small variations of model surface conditions.

RESULTS

The results are presented in this paper without analysis to expedite publication. The variations of drag, nacelle drag increment, pitching moment, and angle of attack with lift coefficient are presented in figures 6 to 12 for a Mach number of 1.60 and a Reynolds number of 2.7×10^6 based on wing mean aerodynamic chord. Data from repeat runs (tailed symbols) are presented in figure 12. Repeat runs were made in order that the check calibration of the drag balance could be further verified and so that data on certain nacelle configurations could be obtained from consecutive tests. No reason for the large discrepancy between the two sets of data for nacelle position 1 is known except that a large number of configurations were tested during the intervening time interval. An attempt was made to fix transition on position 3 nacelles with faired openings and exits (the upstream edge of a 0.25 inch wide band of number 60 carborundum was located approximately 2 percent of the nacelle length from each nacelle tip). The data from this latter run agreed with transition-free data from the previous run and therefore have not been included in this paper. The factor required to convert the nacelle drag increment to a value based on nacelle frontal area is listed in each figure title.

The lift-drag ratios for most of the configurations are presented in figure 13. It is evident from this figure that the nacelle shape and location have only a small effect on the maximum lift-drag ratio. Furthermore, the drag penalty of the thickened root wing-body configuration becomes small when the use of submerged nacelles is considered.

Representative schlieren pictures are presented in figure 14.

Langley Aeronautical Laboratory
National Advisory Committee for Aeronautics
Langley Field, Va.

REFERENCES

1. Bielat, Ralph P., Harrison, Daniel E., and Coppolino, Domenic A.: An Investigation at Transonic Speeds of the Effects of Thickness Ratio and of Thickened Root Sections on the Aerodynamic Characteristics of Wings with 47° Sweepback, Aspect Ratio 3.5, and Taper Ratio 0.2 in the Slotted Test Section of the Langley 8-Foot High-Speed Tunnel. NACA RM L51I04a, 1951.
2. Robinson, Ross B., and Driver, Cornelius: Aerodynamic Characteristics at Supersonic Speeds of a Series of Wing-Body Combinations Having Cambered Wings with an Aspect Ratio of 3.5 and a Taper Ratio of 0.2. Effects of Sweep Angle and Thickness Ratio on the Aerodynamic Characteristics in Pitch at $M = 1.60$. NACA RM L51K16a, 1951.
3. Spearman, M. Leroy, and Hilton, John H., Jr.: Aerodynamic Characteristics at Supersonic Speeds of a Series of Wing-Body Combinations Having Cambered Wings with an Aspect Ratio of 3.5 and a Taper Ratio of 0.2. Effects of Sweep Angle and Thickness Ratio on the Static Lateral Stability Characteristics at $M = 1.60$. NACA RM L51K15a, 1951.
4. Cooper, Morton, Smith, Norman F., and Kainer, Julian H.: A Pressure-Distribution Investigation of a Supersonic Aircraft Fuselage and Calibration of the Mach Number 1.59 Nozzle of the Langley 4-by 4-Foot Supersonic Tunnel. NACA RM L9E27a, 1949.
5. Baals, Donald D., Smith, Norman F., and Wright, John B.: The Development and Application of High-Critical-Speed Nose Inlets. NACA Rep. 920, 1948. (Formerly NACA ACR L5F30a)

TABLE I
 AIRFOIL COORDINATES FOR THE 6-PERCENT-THICK AND
 THICKENED ROOT WINGS

[Thickness distribution: NACA 65A series. Mean line ordinates:
 $1/3$ of NACA 230 + ($a = 1$) for $C_L = 0.1$]

6-percent-thick wing

x/c	y/c	y/c
	Upper surface	Lower surface
0	0.061	0
.5	.577	.376
.75	.717	.446
1.25	.919	.534
2.5	1.304	.621
5.0	1.872	.761
7.5	2.318	.857
10	2.668	.980
15	3.150	1.269
20	3.482	1.496
25	3.701	1.697
30	3.858	1.846
35	3.946	1.960
40	3.981	2.021
45	3.937	2.030
50	3.823	1.977
55	3.613	1.872
60	3.342	1.697
65	3.018	1.487
70	2.651	1.277
75	2.231	1.059
80	1.785	.849
85	1.339	.639
90	.892	.420
95	.446	.210
100	0	0

L.E. radius = 0.0024c

Thickened root wing

x/c	Root station	
	y/c	y/c
	Upper surface	Lower surface
0	0.301	0
.5	1.120	.754
.75	1.335	.904
1.25	1.658	1.141
2.5	2.261	1.507
5.0	3.208	2.024
7.5	3.919	2.433
10	4.500	2.799
15	5.362	3.445
20	5.965	3.984
25	6.395	4.414
30	6.718	4.716
35	6.912	4.910
40	6.977	5.017
45	6.912	4.996
50	6.675	4.823
55	6.288	4.522
60	5.771	4.113
65	5.168	3.618
70	4.457	3.101
75	3.725	2.584
80	2.929	2.067
85	2.239	1.550
90	1.486	1.034
95	.732	.517
100	0	0

L.E. radius = 0.0099c

TABLE II

TABULATION OF WING AND NACELLE CONFIGURATIONS TESTED AND
FIGURE NUMBERS IN WHICH BASIC DATA ARE PRESENTED

Wing thickness (percent)	Nacelle position	Nacelle nose	Nacelle afterbody	Figure in which basic data are presented	
6	None	-----	-----	6,8,10,12	
12 to 6	None	-----	-----	11	
6	Submerged	Faired	Faired	10	
12 to 6	Submerged	Faired	Faired	11	
6	1	Faired	Faired	6,12	
Consecutive tests	6	3	Faired	Faired	6,8
	6	3	1-66-100	1-66-050	8,12
	6	2	Faired	Faired	6
	6	4	Faired	Faired	6
Consecutive tests	6	1	1-66-100	1-66-050	9
	6	1	Faired	Faired	9,12
	6	1	1-60-300	1-66-050	9
Consecutive tests	6	None	-----	-----	7,9,12
	6	3	1-60-300	1-66-050	7
	6	3	1-66-050	1-66-050	7
	6	3	1-66-100	1-66-050	7,12



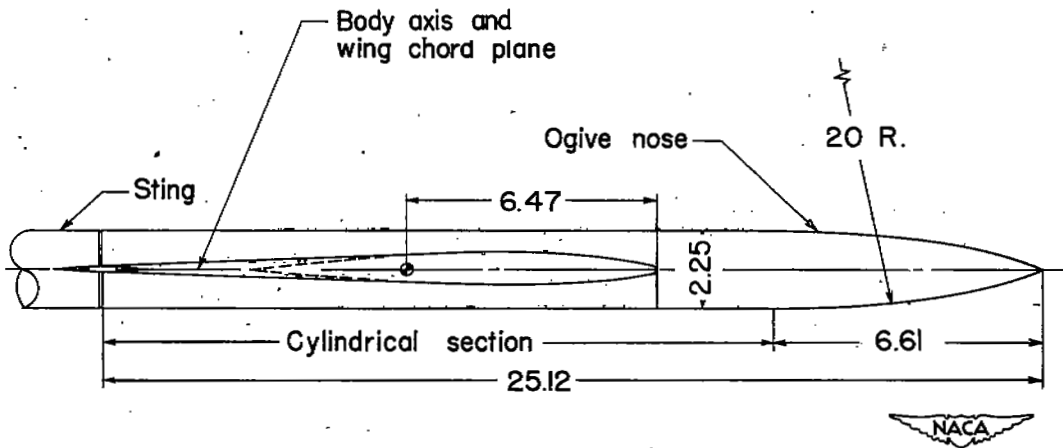
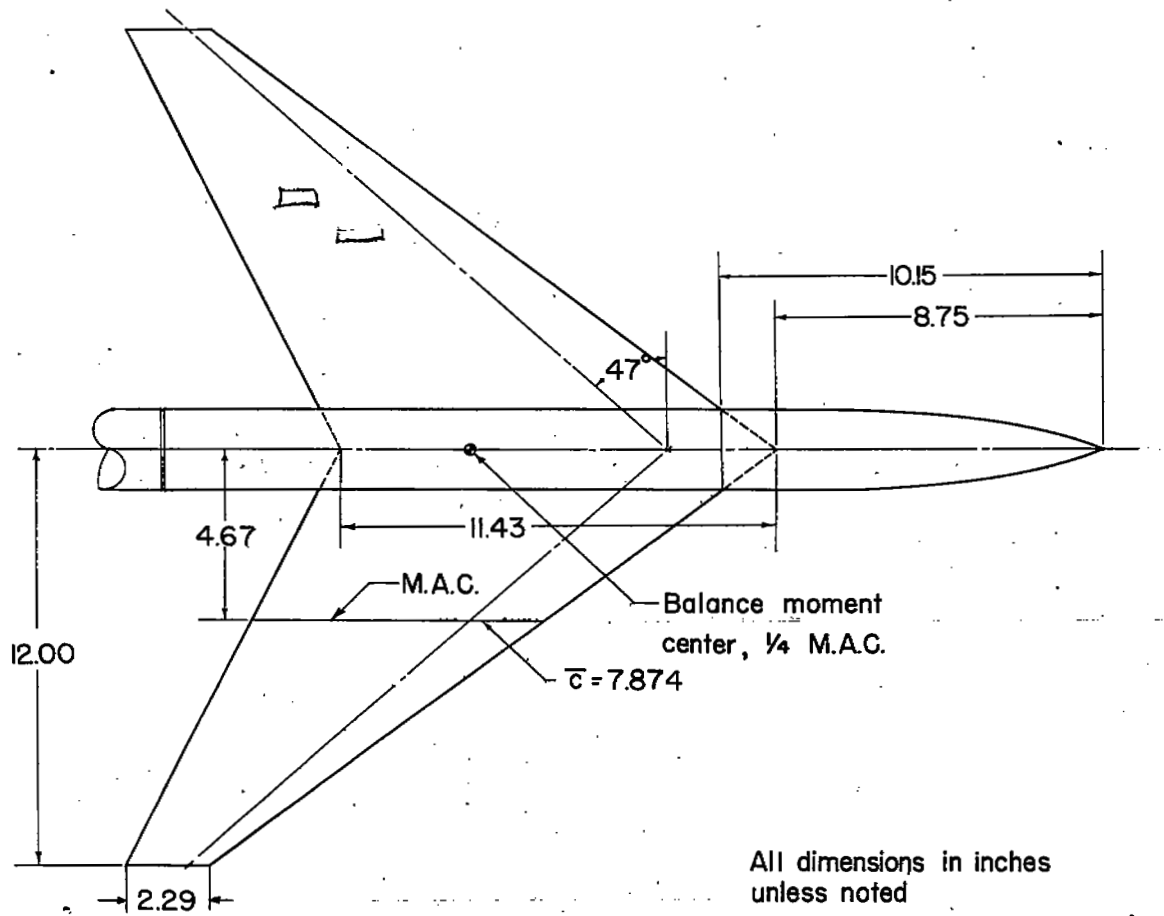
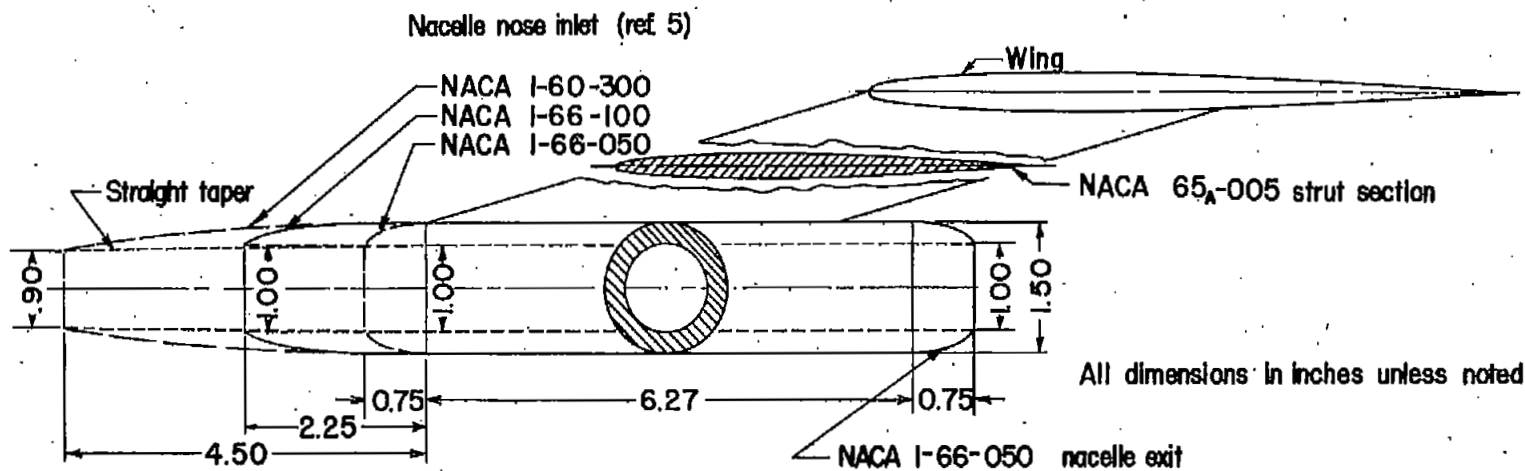
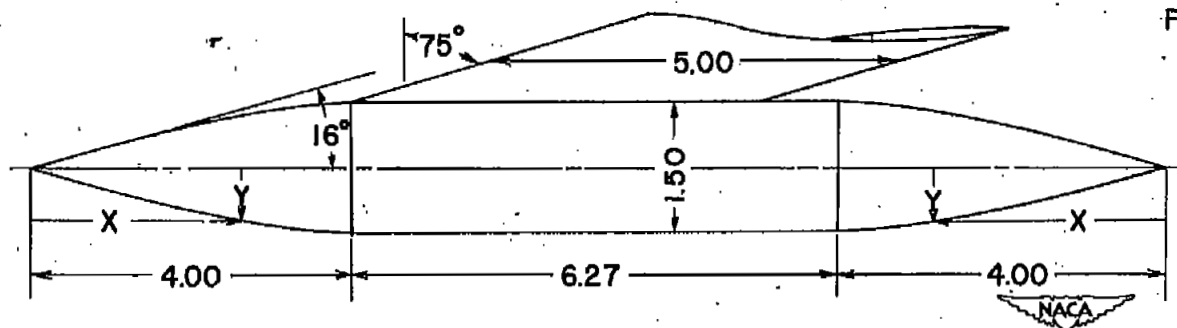


Figure 1.- Details of body and 47° sweptback wing.



(a) Open nacelles.



Faired nacelle coordinates

X	Y
0	0
1.00	.287
1.50	.422
2.00	.536
2.50	.626
3.00	.693
3.50	.735
4.00	.750

(b) Faired nacelle.

Figure 2.- Details of open and faired nacelles, and nacelle strut.

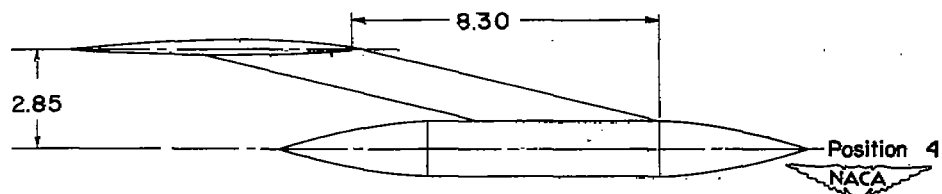
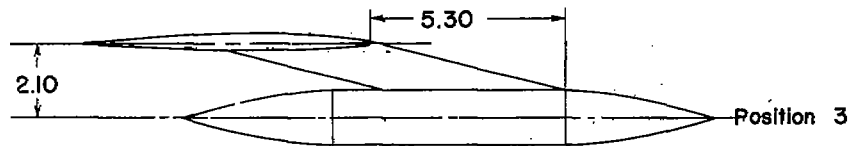
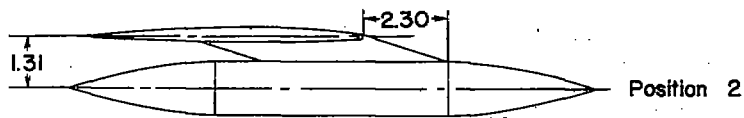
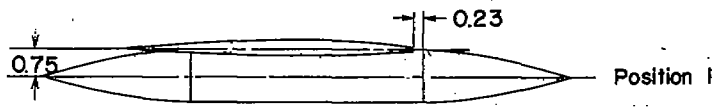
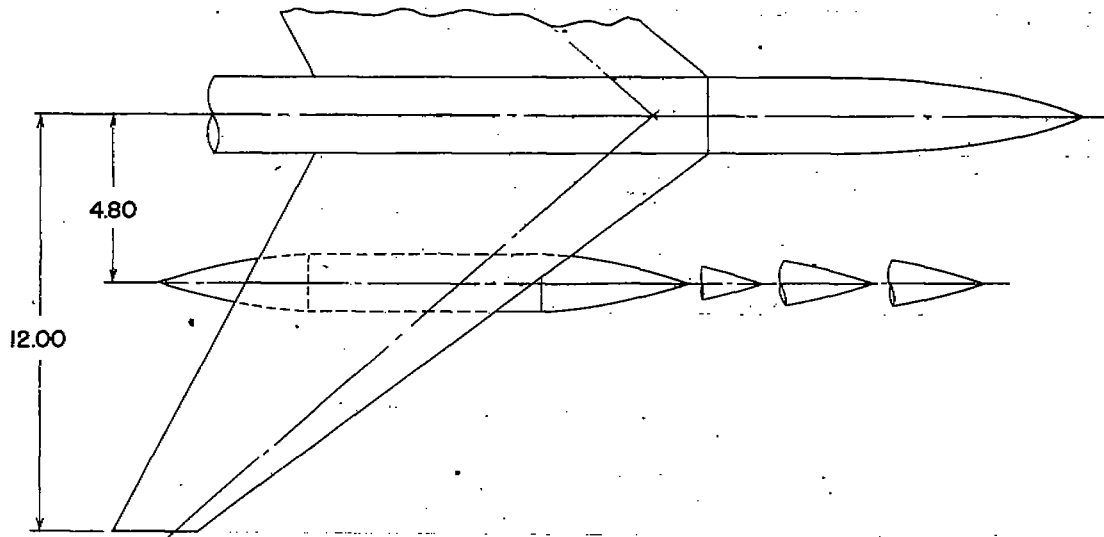
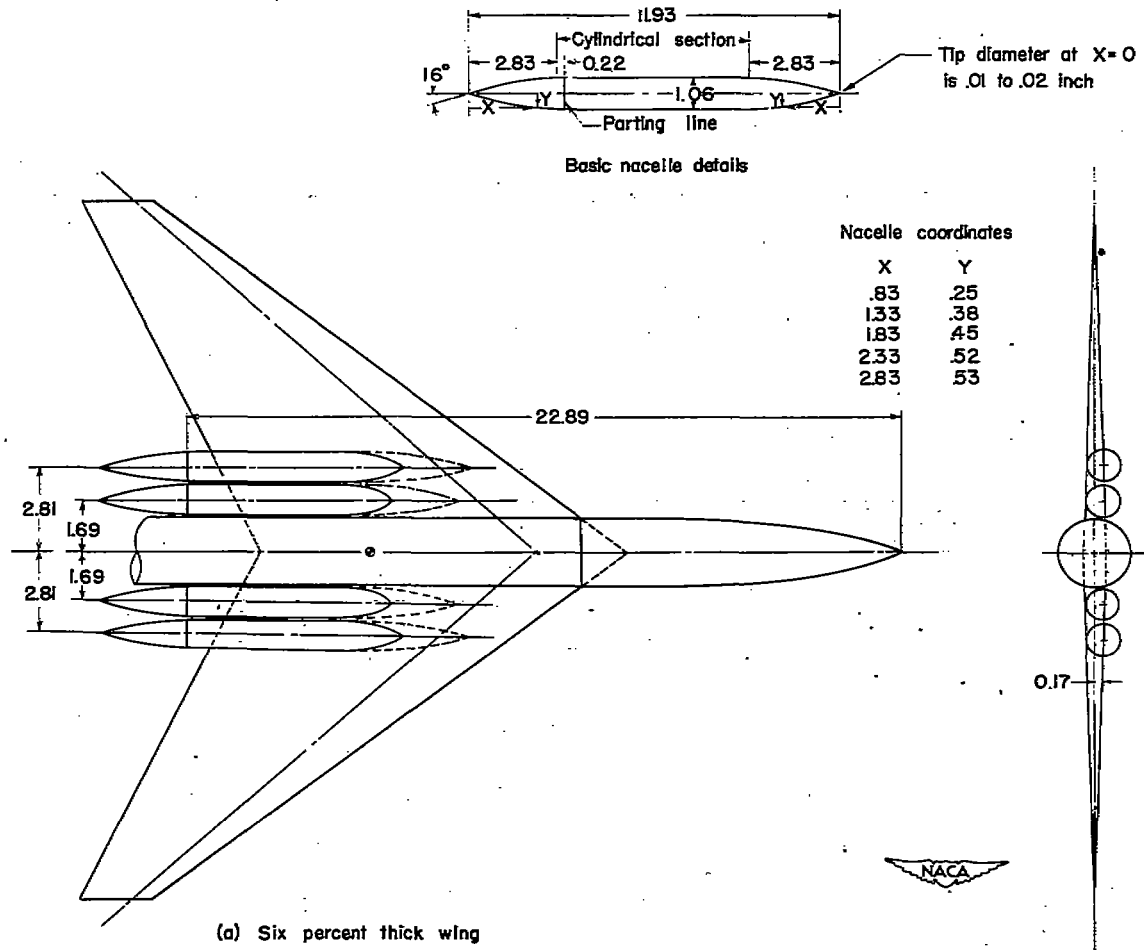
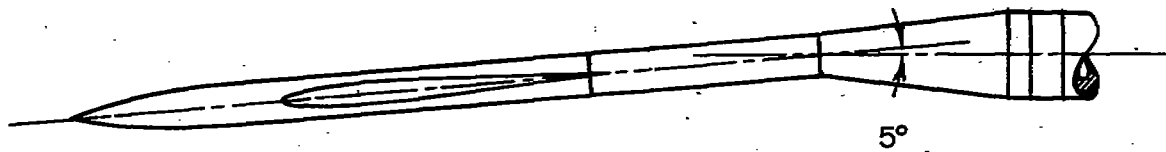


Figure 3.- Nacelle position designation.

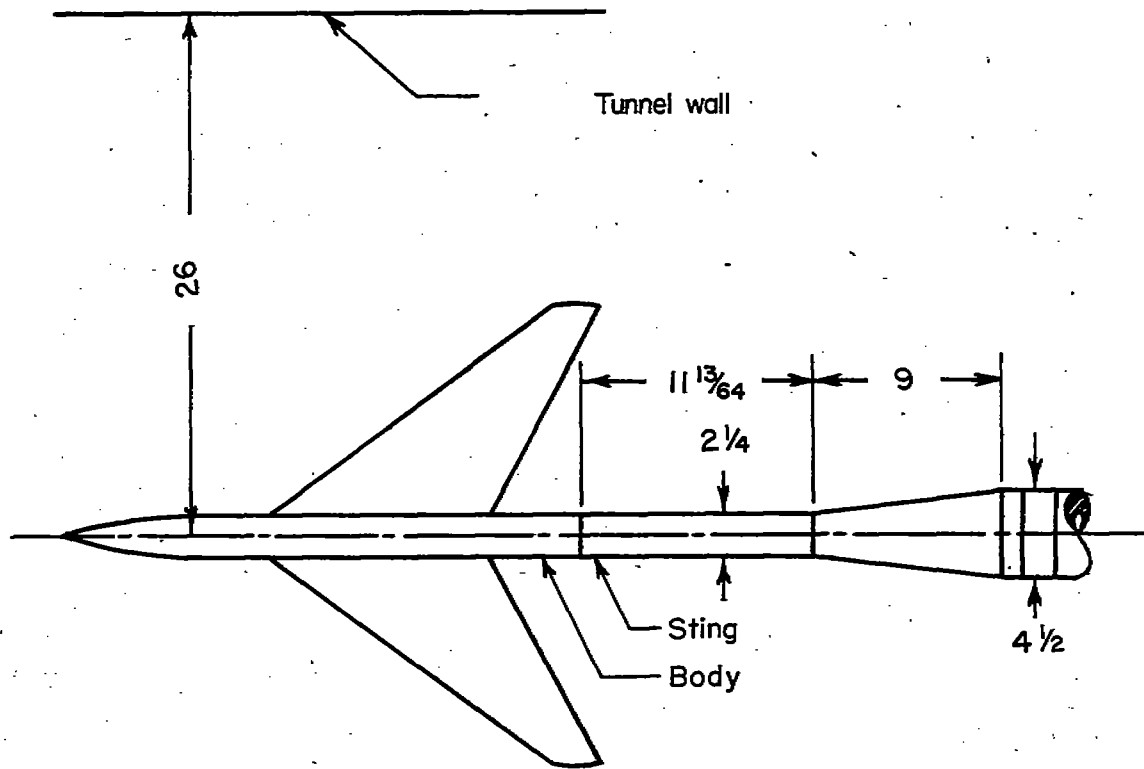


(a) 6-percent-thick wing.

Figure 4.- Details of submerged nacelles and nacelle locations on wings.
All dimensions in inches unless noted.



Top view of installation



Side view of installation



Figure 5.- Details of model sting support. All dimensions in inches unless noted.

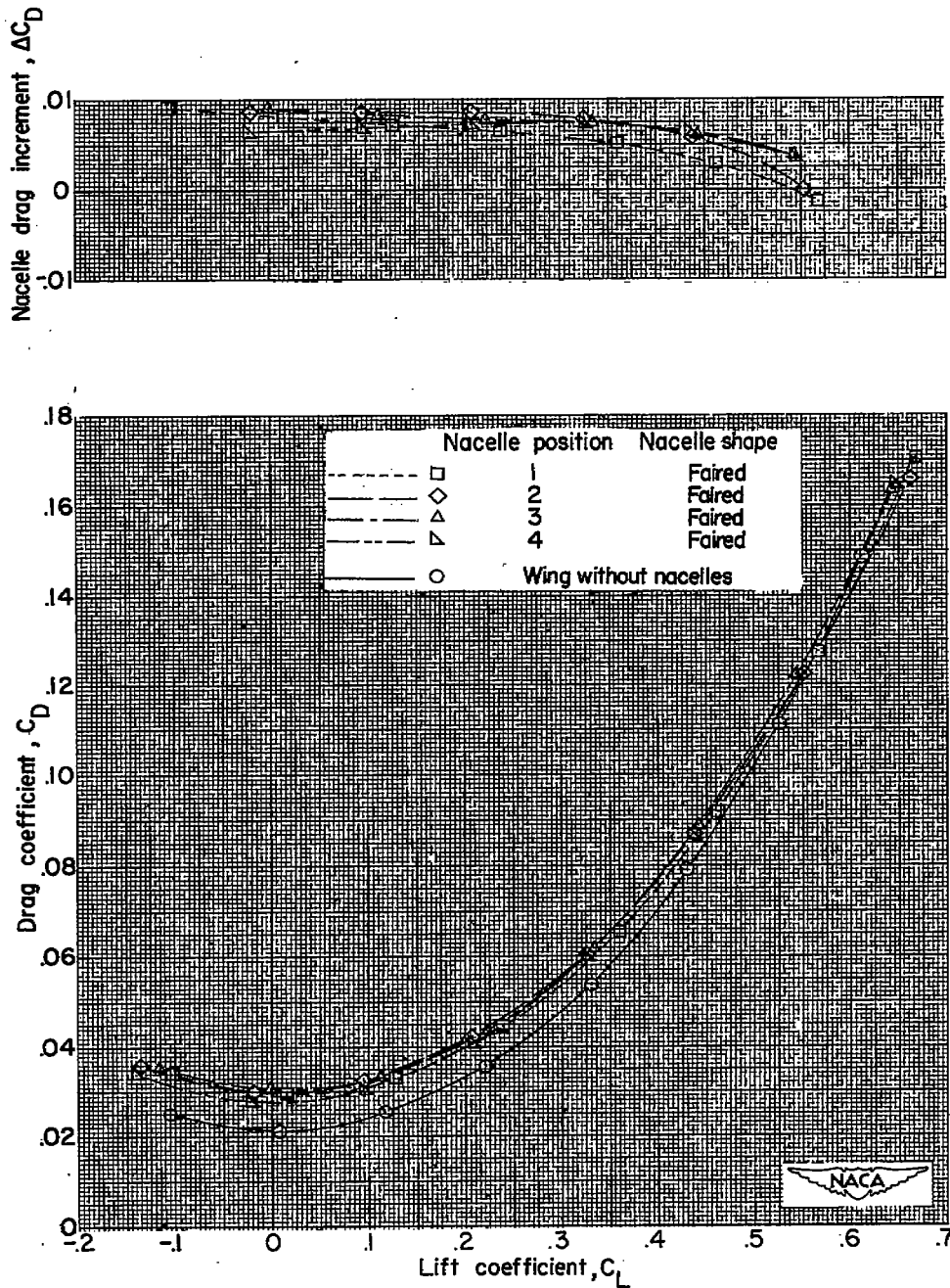


Figure 6.- Effect of position of strut-mounted faired nacelles on the aerodynamic characteristics in pitch of the 6-percent-thick wing-body combination. The ratio of wing-plan-form area to the frontal area of the two nacelles is 46.57.

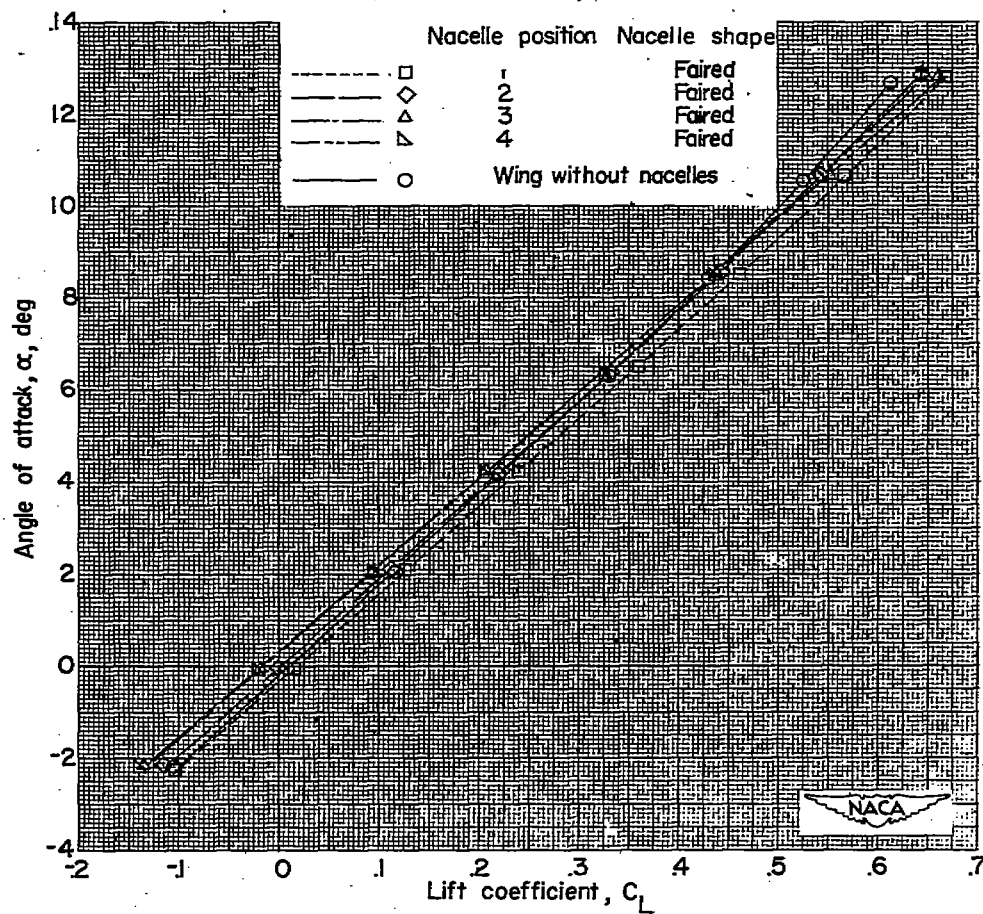
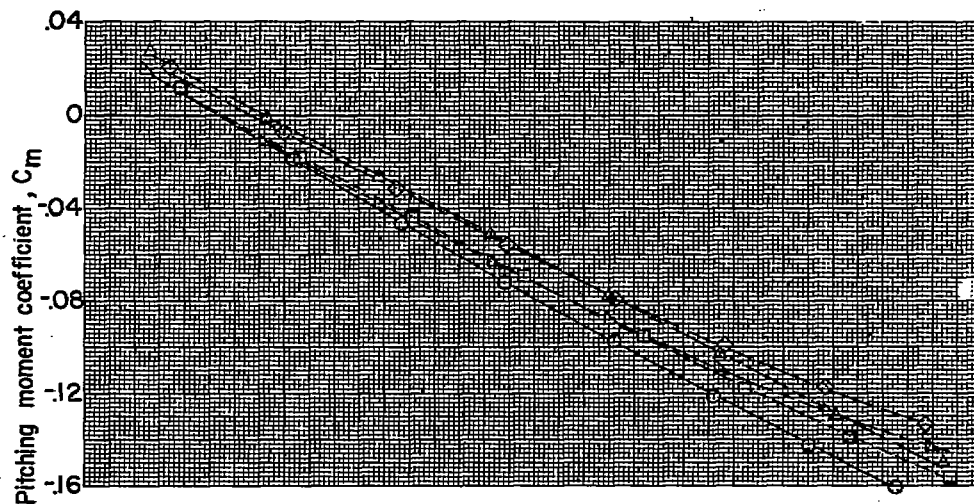


Figure 6.- Concluded.

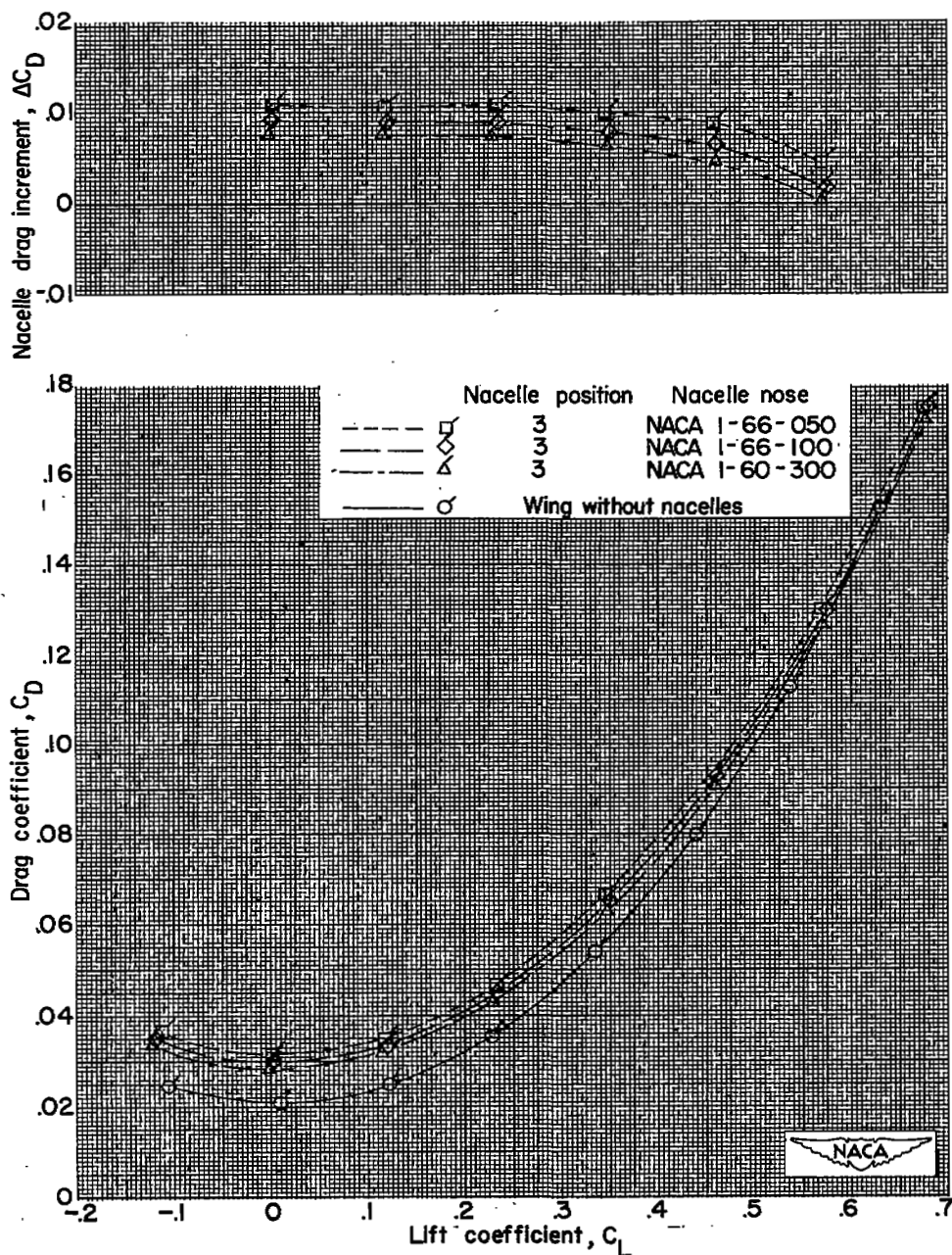


Figure 7.- Effect of various nacelle nose configurations on the aerodynamic characteristics in pitch of the 6-percent-thick wing-body combination with the nacelles mounted at position 3. The ratio of wing-plan-form area to the frontal area of the two nacelles is 46.57.

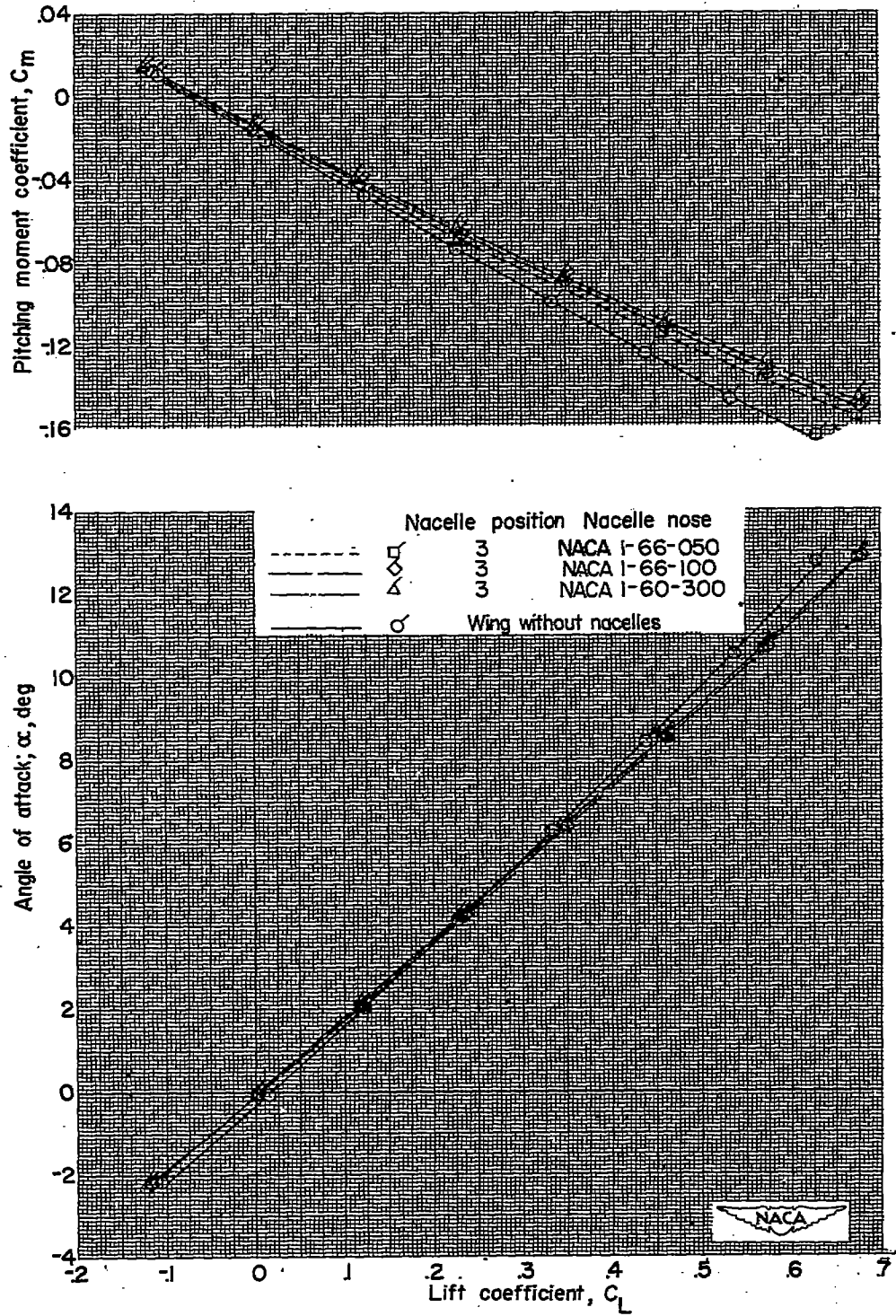


Figure 7.- Concluded.

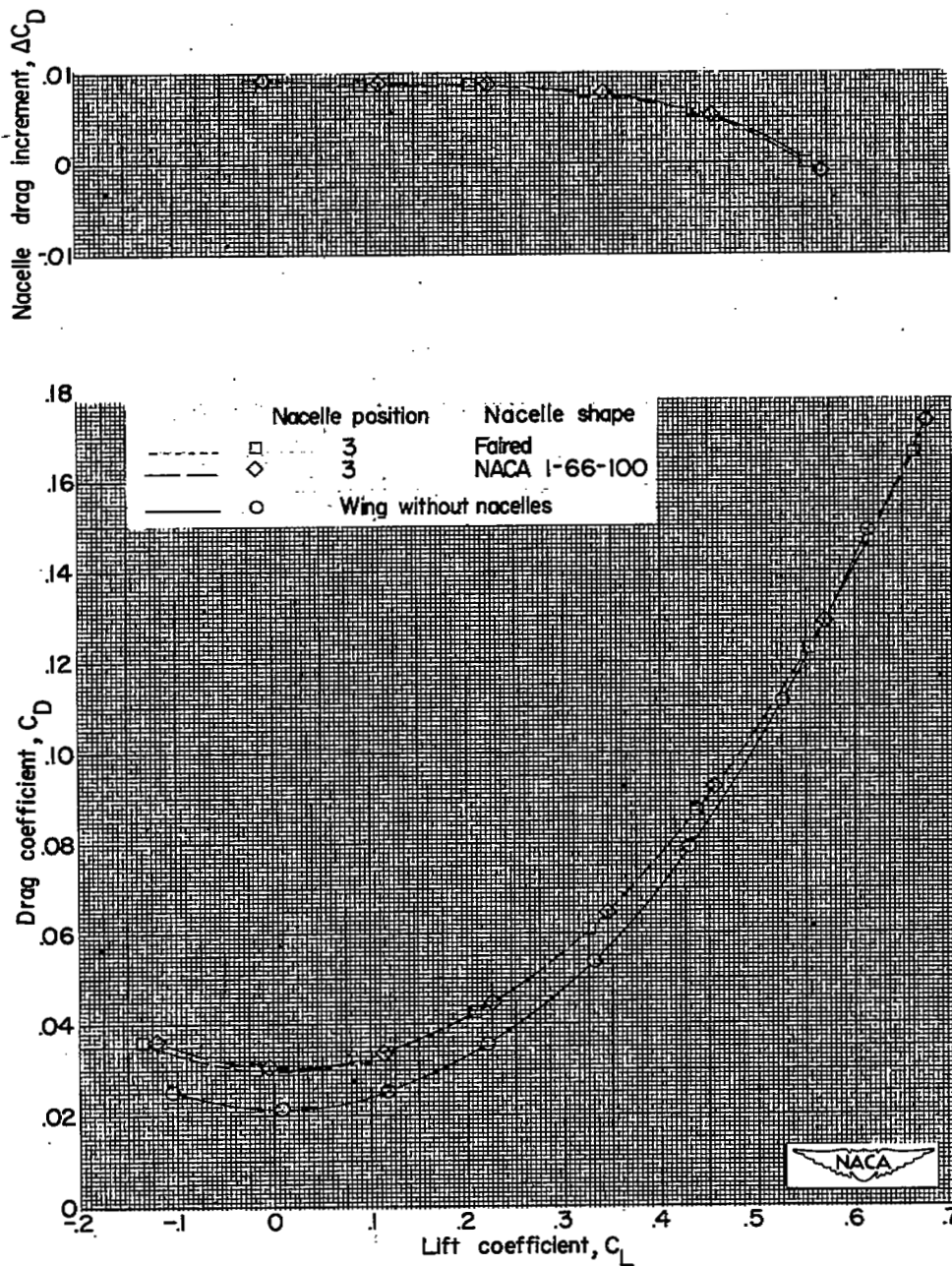


Figure 8.- Effect of nacelle shape on the aerodynamic characteristics in pitch of the 6-percent-thick wing-body combination with the nacelles mounted at position 3. The ratio of wing-plan-form area to the frontal area of the two nacelles is 46.57.

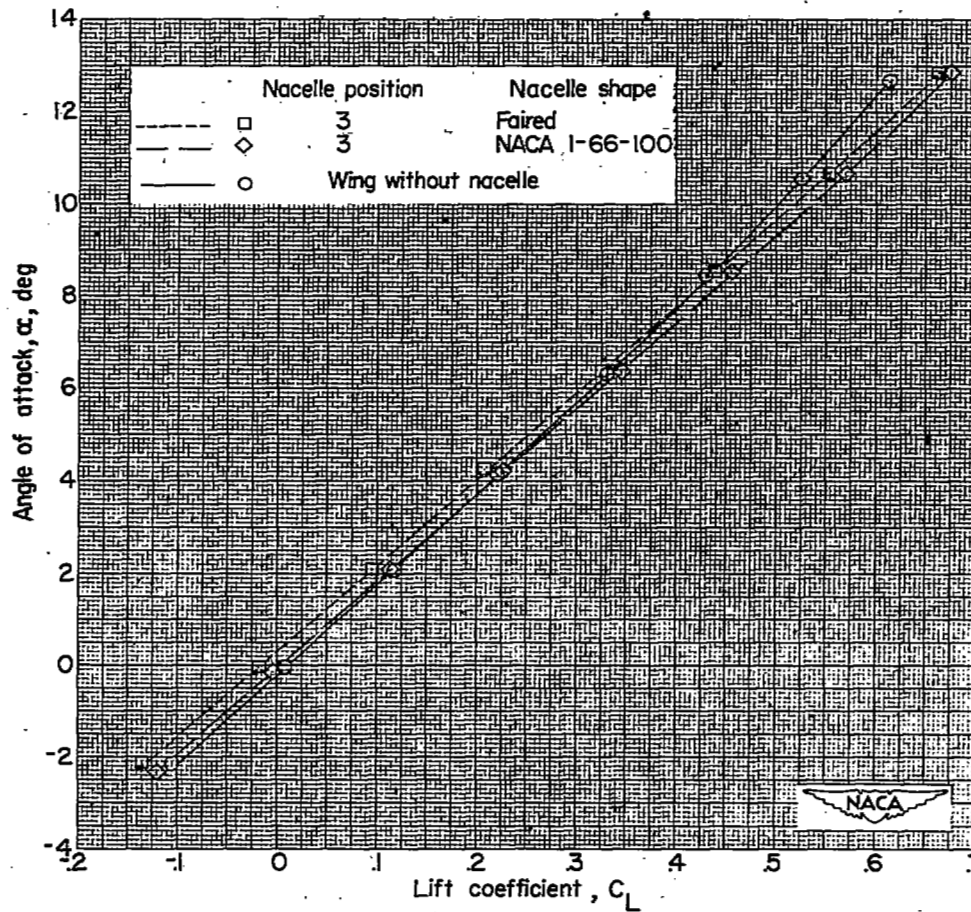
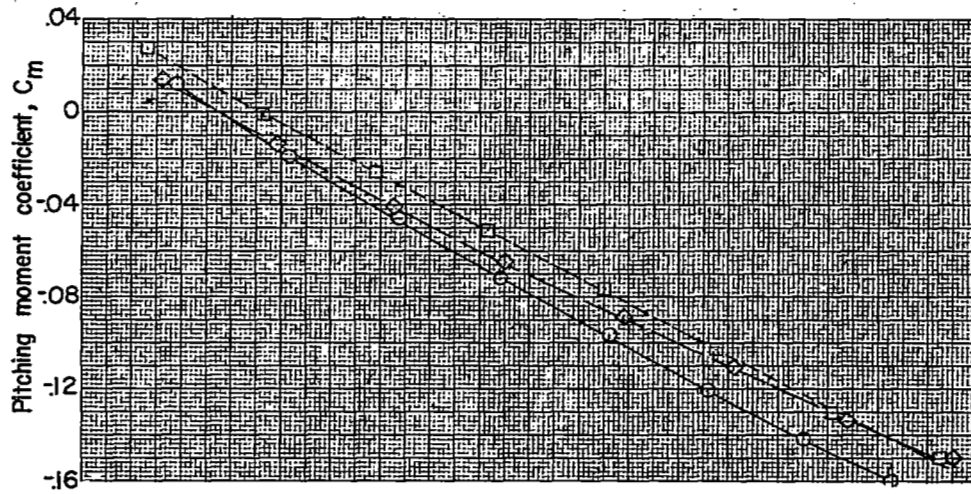


Figure 8.- Concluded.

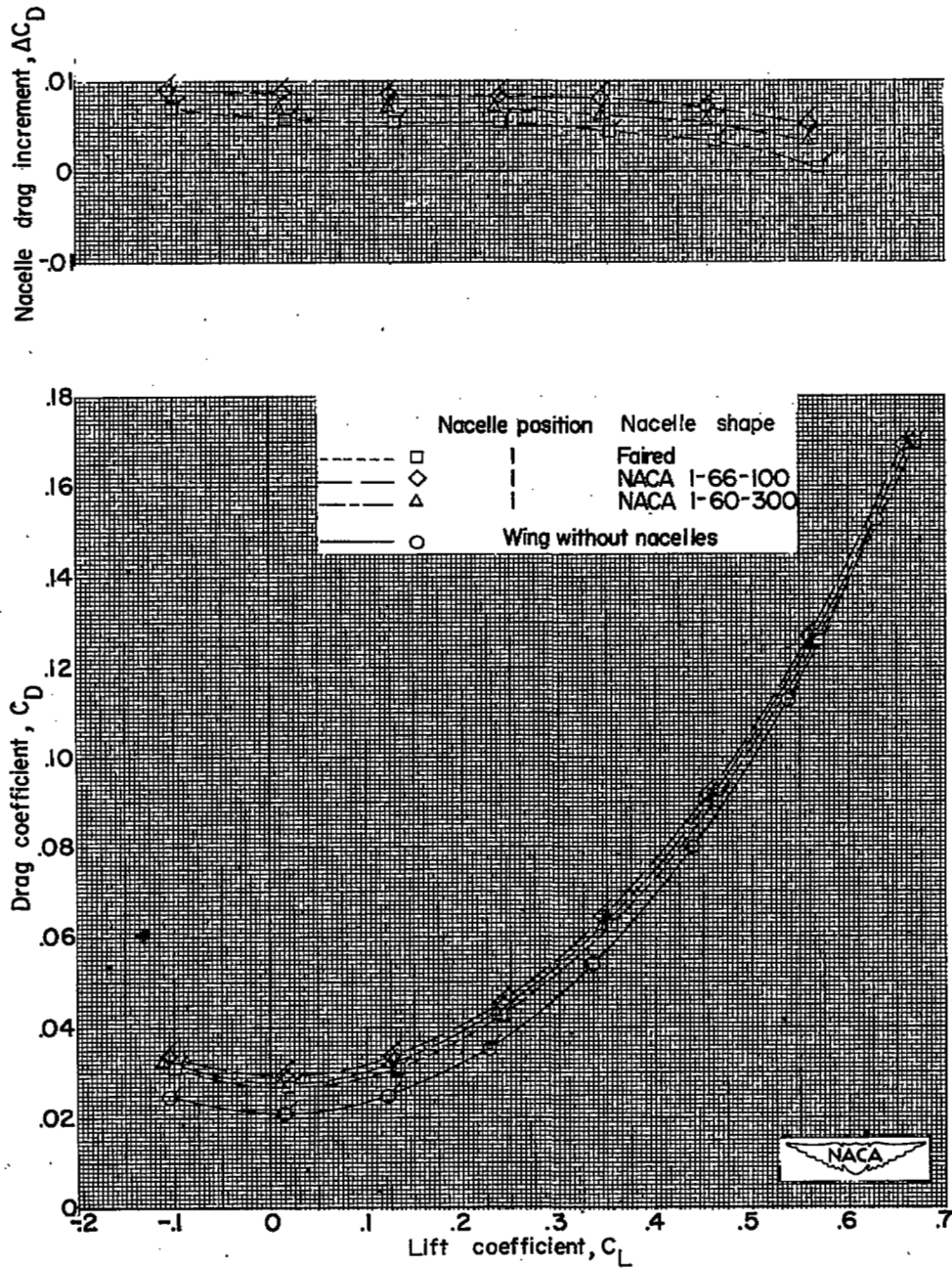
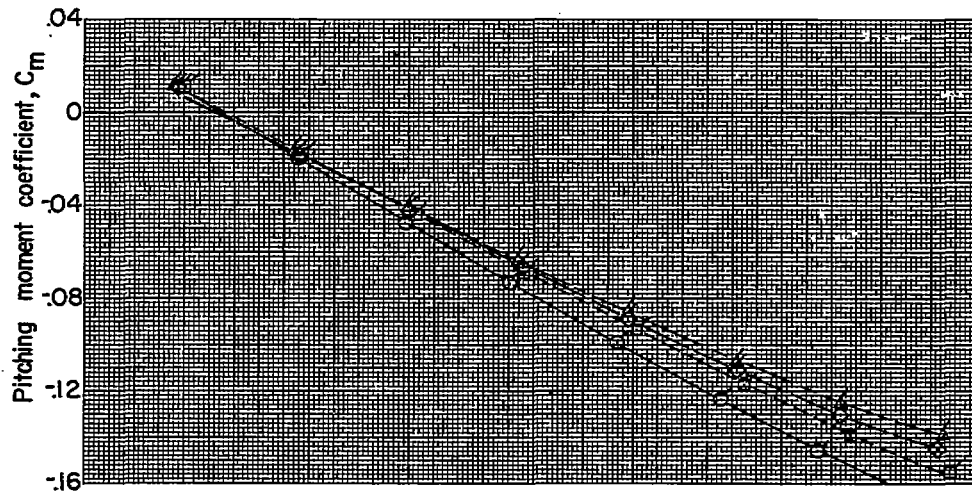
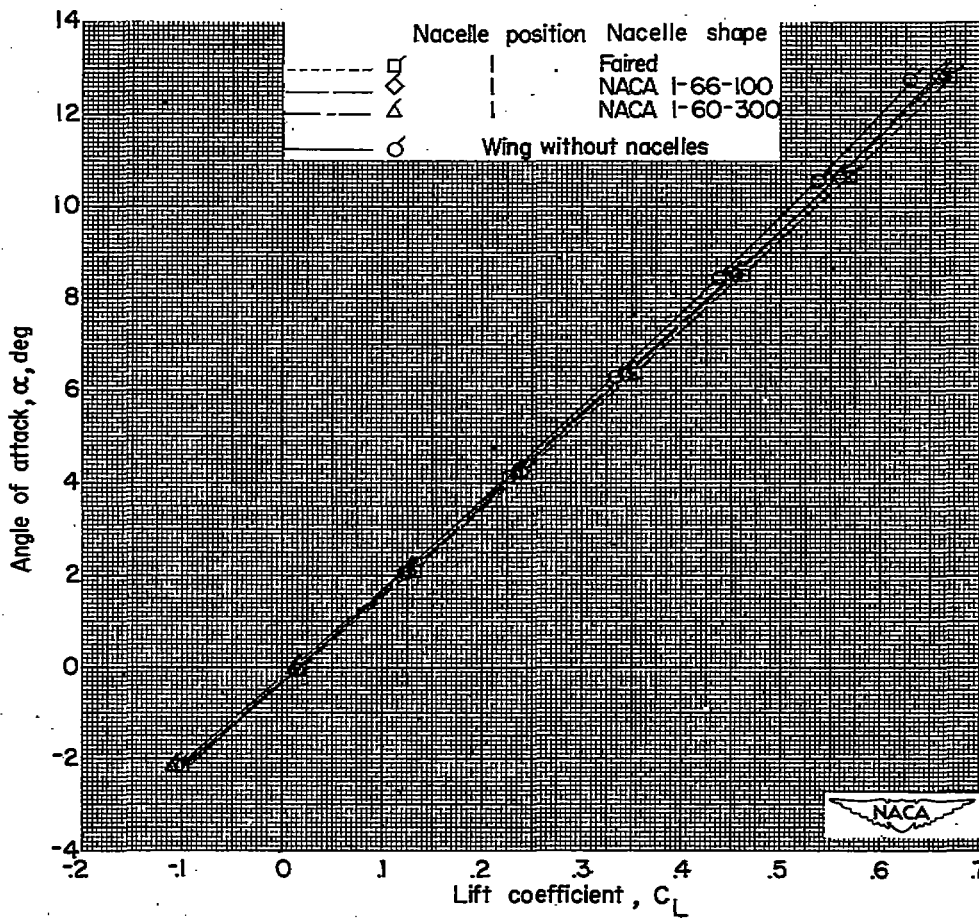


Figure 9.- Effect of various nacelle shapes on the aerodynamic characteristics in pitch of the 6-percent-thick wing-body combination with the nacelles mounted at position 1. The ratio of wing-plan-form area to the frontal area of the two nacelles is 46.57.



$\Delta C_m = \frac{1.157}{0.05}$
 $C_L = 0.05$
 $C_m = \frac{-1.157}{0.05} = -23.14$



$\Delta \alpha = 5$
 $\Delta C_L = \frac{1.264}{0.17}$
 $C_L = 0.17$

Figure 9.- Concluded.

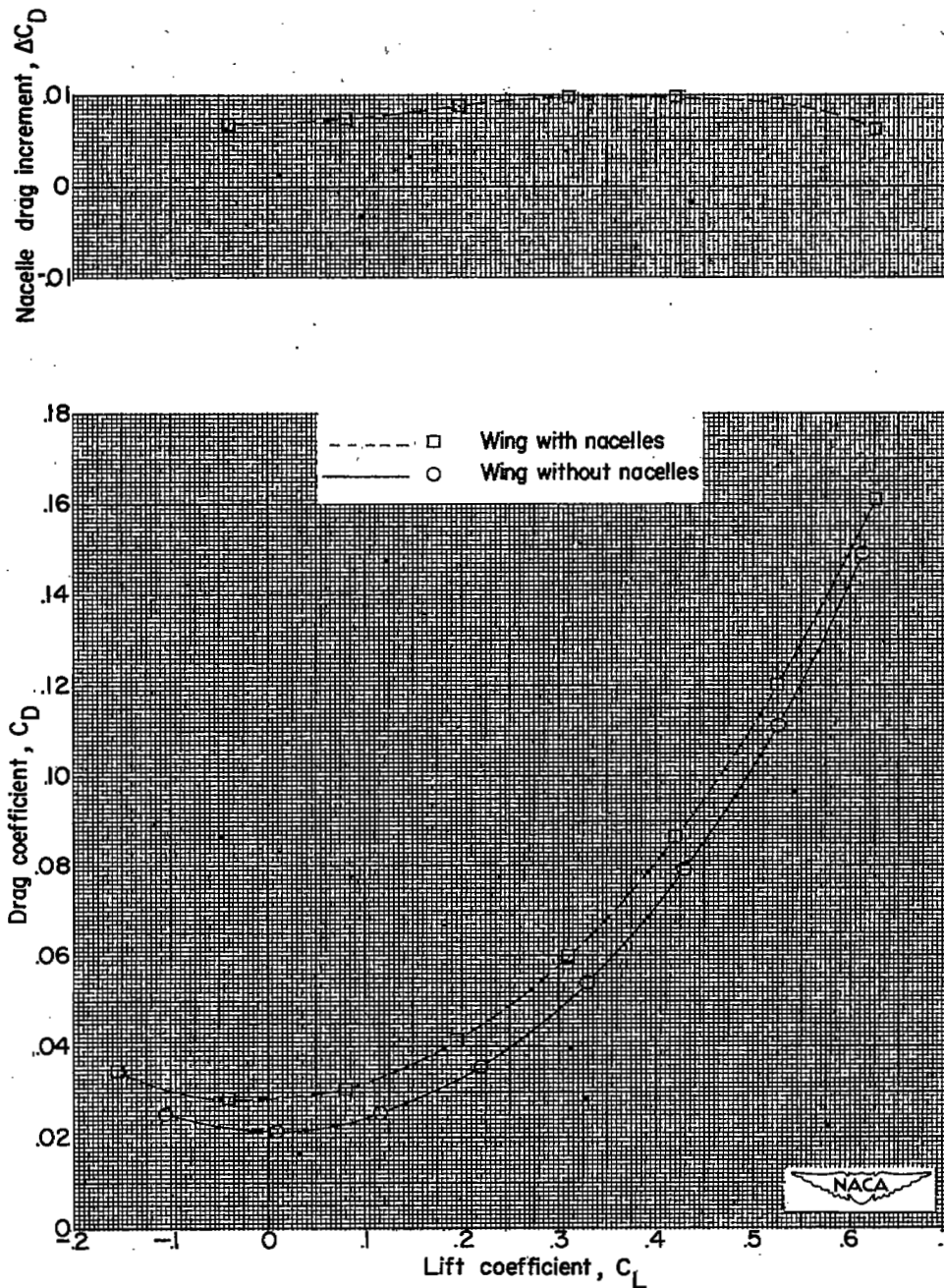


Figure 10.- Effect of paired, submerged nacelles on the aerodynamic characteristics in pitch of the 6-percent-thick wing-body combination. The ratio of wing-plan-form area to the frontal area of the four nacelles is 46.63.

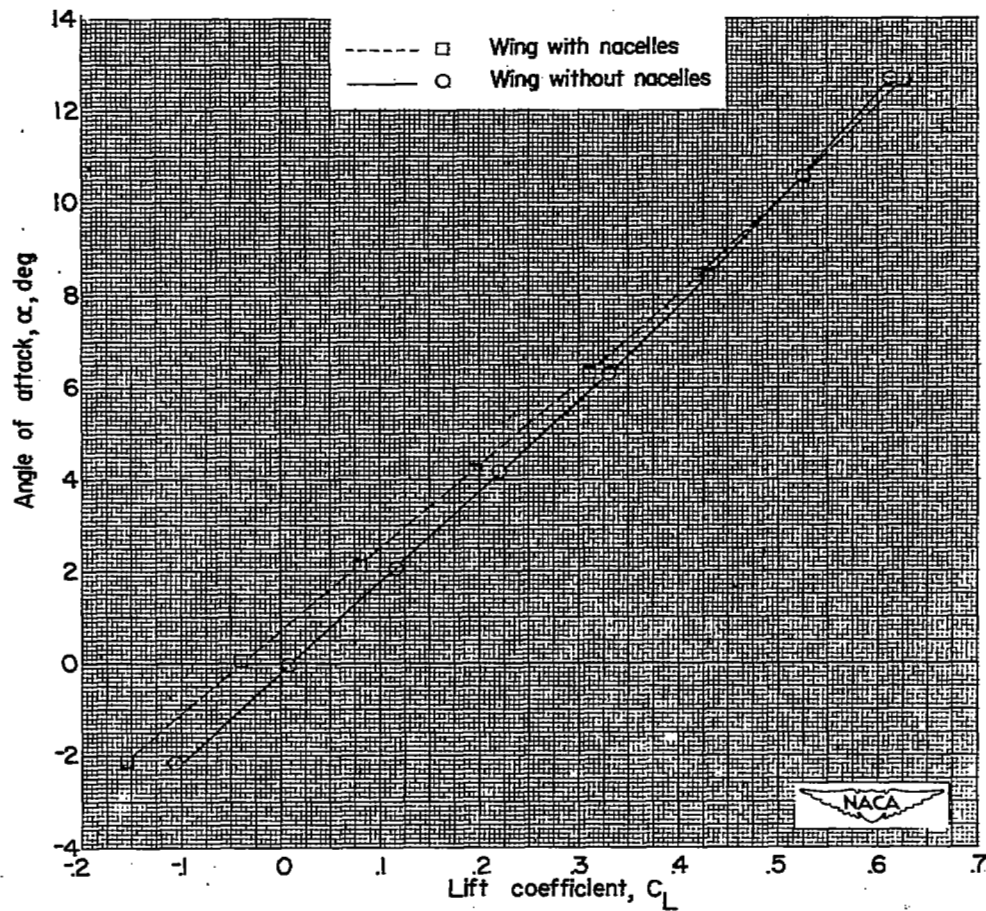
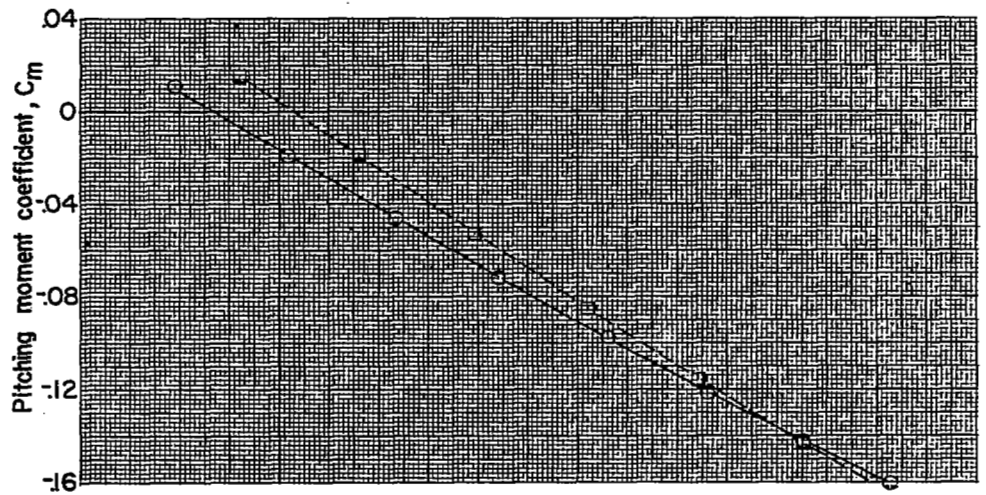


Figure 10.- Concluded.

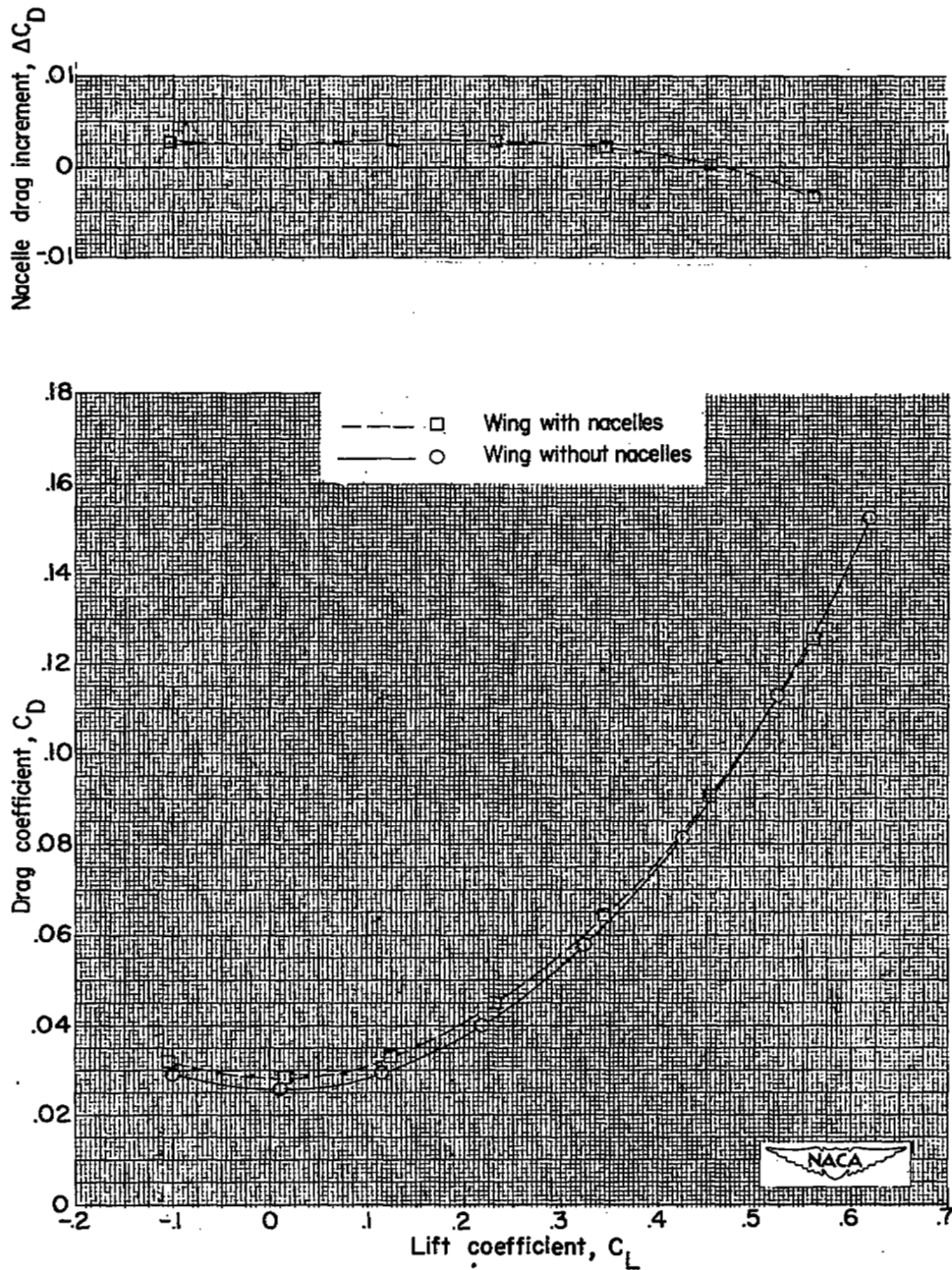


Figure 11.- Effect of faired, submerged nacelles on the aerodynamic characteristics in pitch of the wing-body combination with wing thickness ratio varying from 12 to 6 percent. The ratio of wing-plan-form area to frontal area of the four nacelles is 46.63.

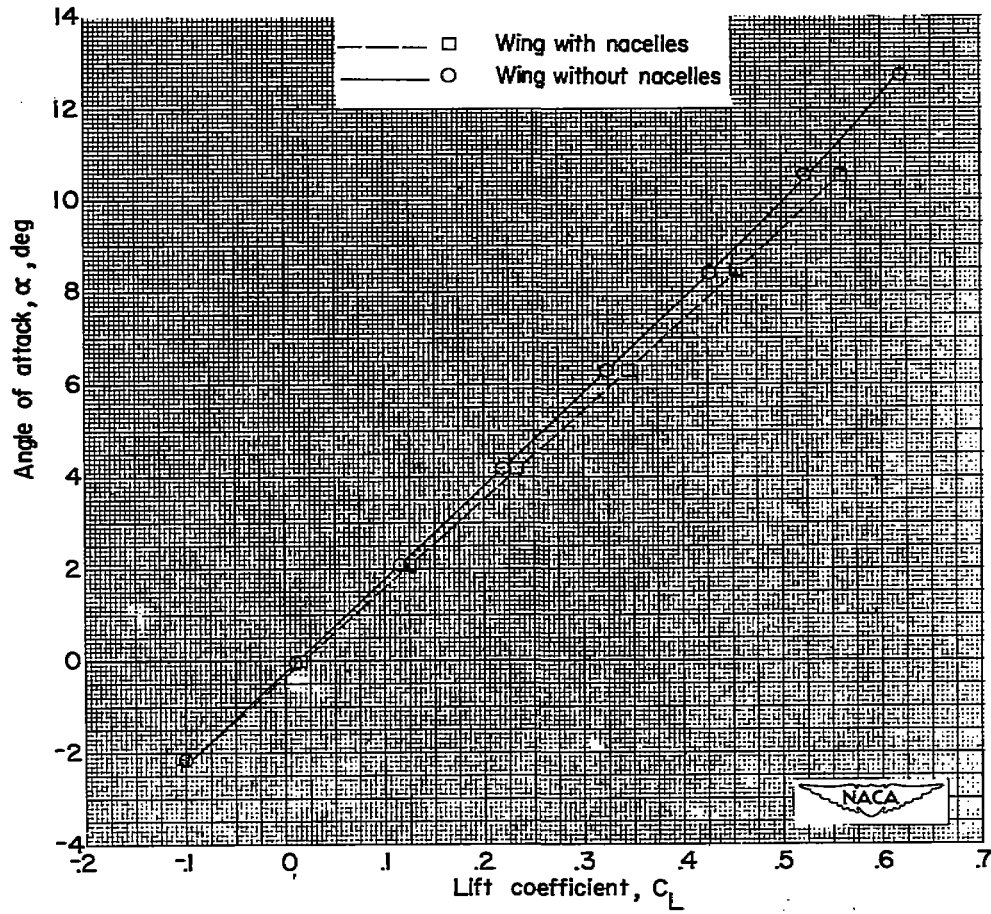
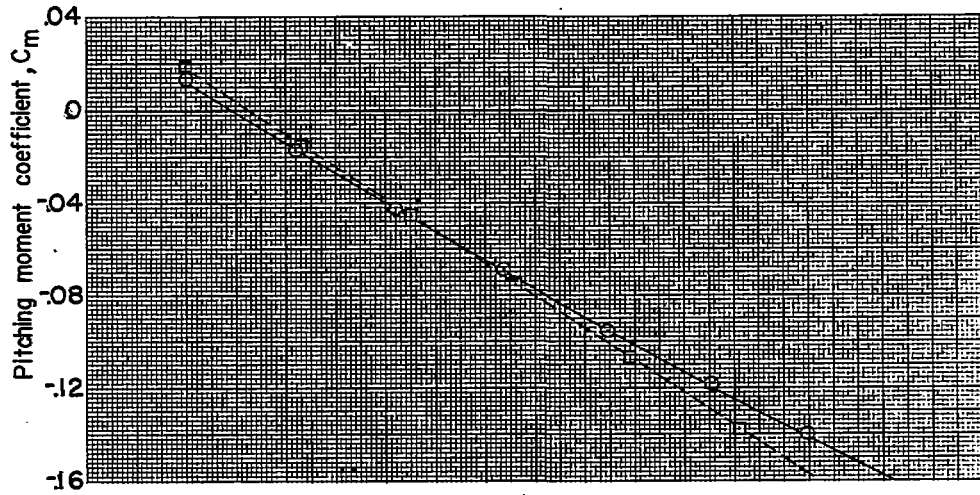


Figure 11.- Concluded.

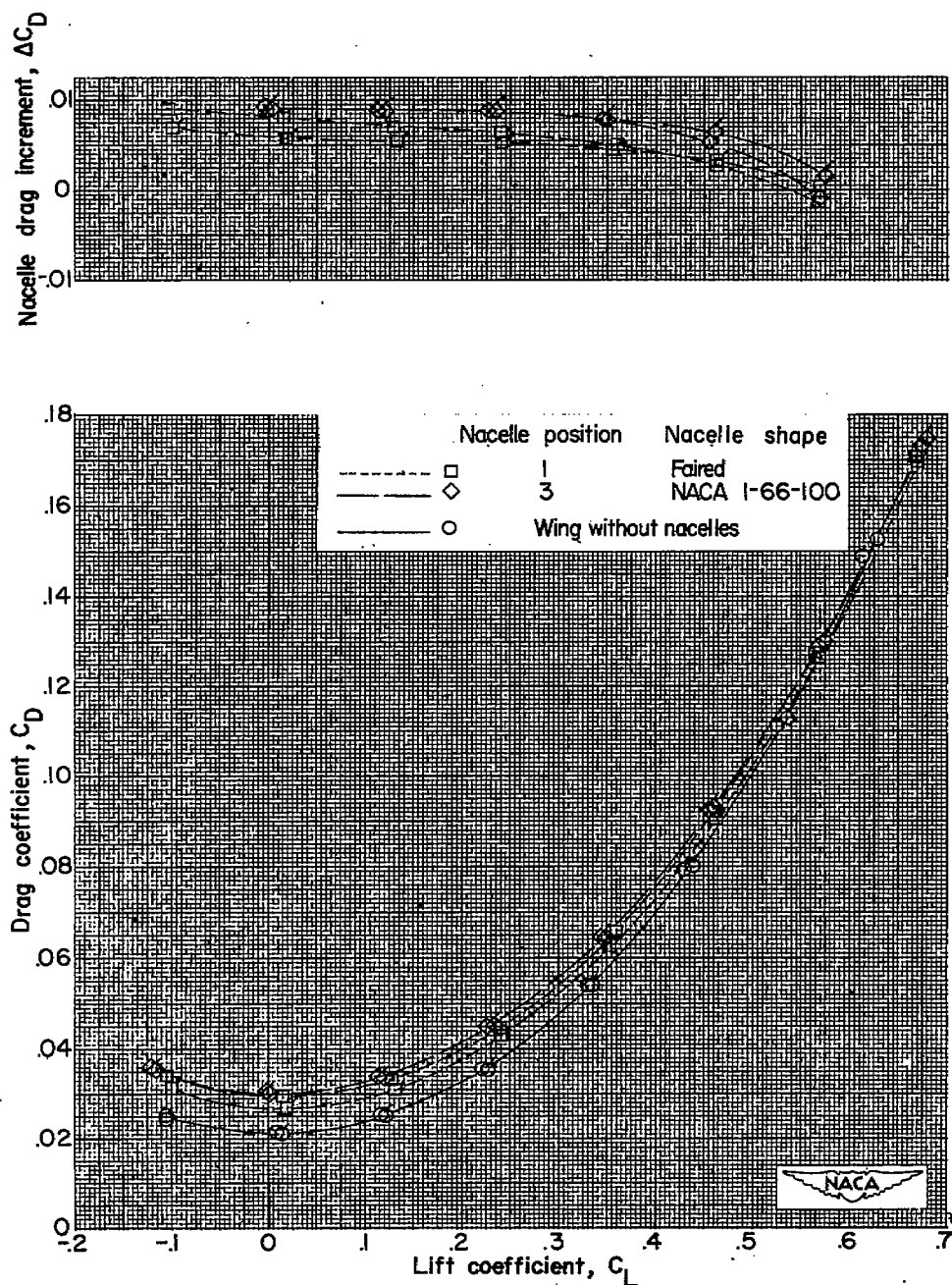


Figure 12.- Comparison of the original and repeat sets (tailed symbols) of data obtained from three model configurations. The ratio of wing plan-form area to the frontal area of the two nacelles is 46.57.

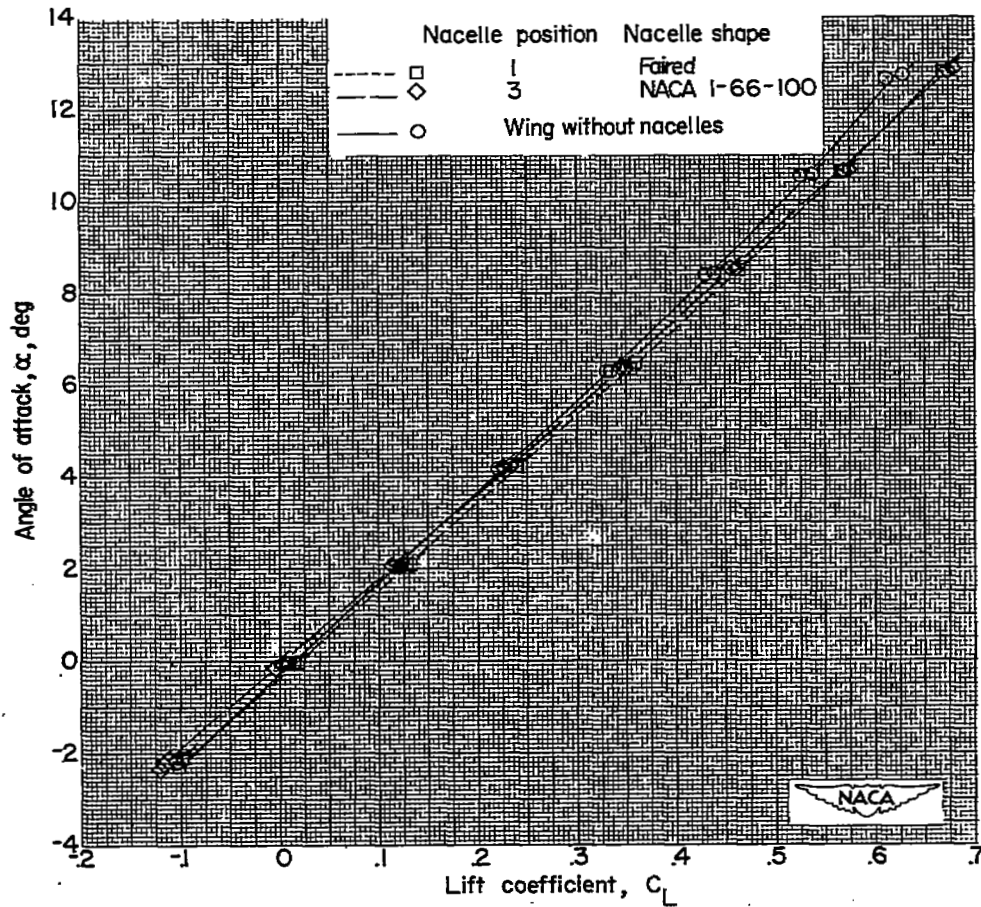
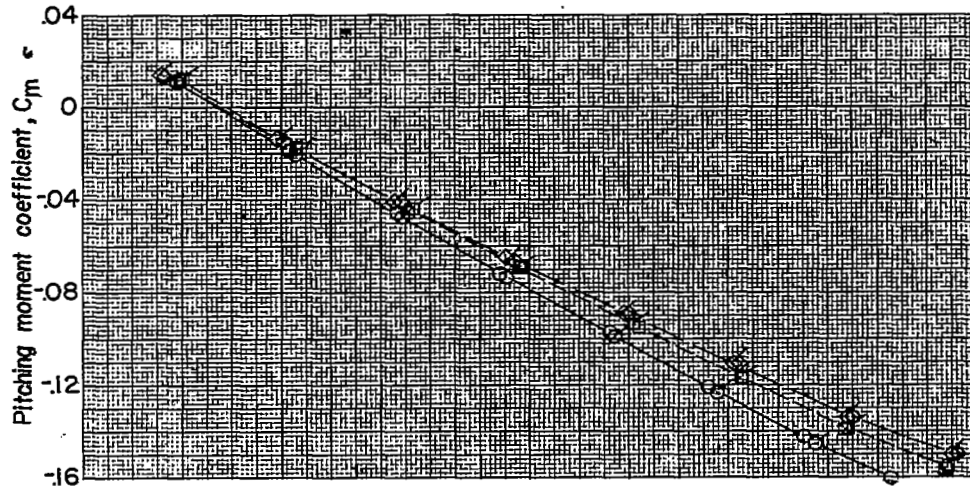


Figure 12.- Concluded.

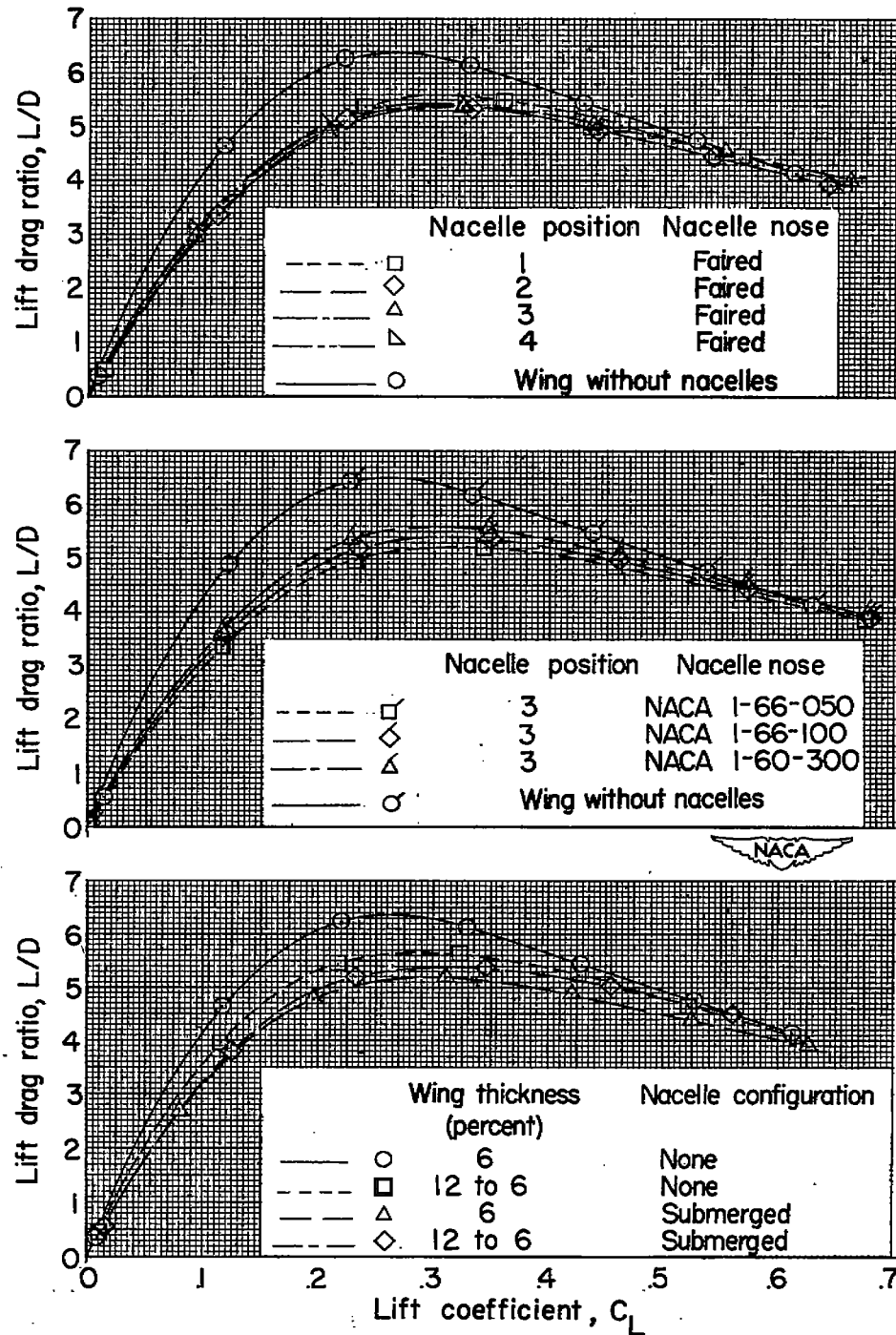
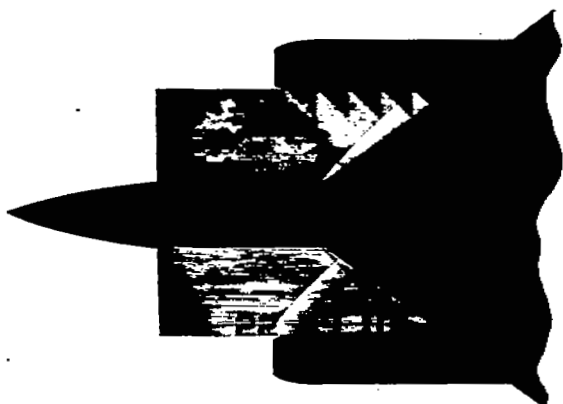
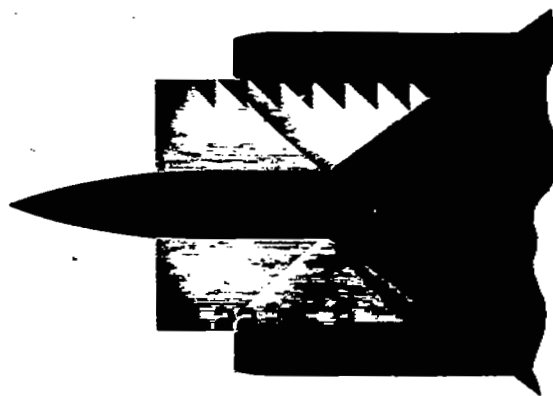
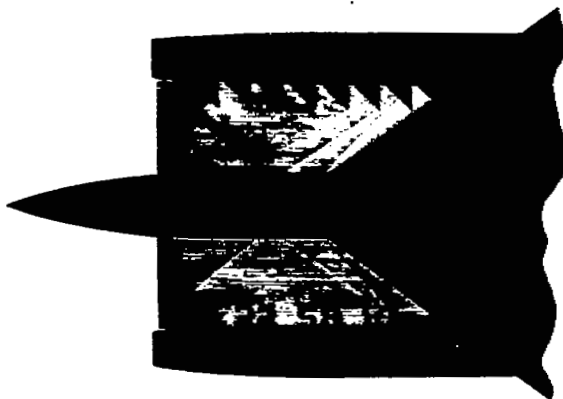
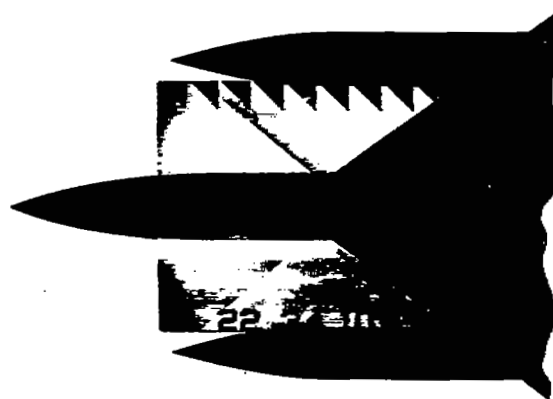
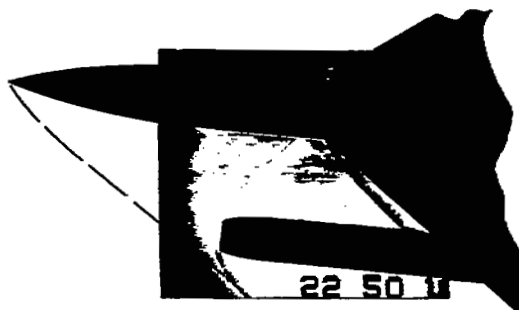


Figure 13.- Variation with lift coefficient of the lift-drag ratios of the 6-percent-thick and thickened root wing-body combinations with and without nacelles.

(a) NACA 1-66-050 nose inlet; $\psi = 0^\circ$.(b) NACA 1-66-100 nose inlet; $\psi = 0^\circ$.(c) NACA 1-60-300 nose inlet; $\psi = 0^\circ$.(d) Faired inlet; $\psi = 0^\circ$.(e) NACA 1-66-100 nose inlet; $\psi = 5^\circ$.

NACA
L-70846

Figure 14.- Schlieren photographs of open and faired nacelles mounted at position 3 on the 6-percent-thick wing. $\alpha = 0^\circ$.

~~SECURITY INFORMATION~~

~~CONFIDENTIAL~~

LANGLEY RESEARCH CENTER

3 1176 00508 9454



~~CONFIDENTIAL~~